Original Research Paper

Alginate encapsulated mesoporous silica nanospheres as a sustained drug delivery system for the poorly water-soluble drug indomethacin

Liang Hu [a], Changshan Sun [a], Aihua Song [b], Di Chang [a], Xin Zheng [c], Yikun Gao [a], Tongying Jiang [a], Siling Wang [a,]*

[a] *Department of Pharmaceutics, Shenyang Pharmaceutical University, P.O. Box 32, Liaoning Province, Shenyang 110016, China*
[b] *Testing Center in School of Pharmacy, Shenyang Pharmaceutical University, Shenyang 110016, China*
[c] *School of Pharmaceutical Engineering, Shenyang Pharmaceutical University, Shenyang 110016, China*

A R T I C L E   I N F O

A B S T R A C T

We applied a combination of inorganic mesoporous silica material, frequently used as drug carriers, and a natural organic polymer alginate (ALG), to establish a sustained drug delivery system for the poorly water-soluble drug Indomethacin (IND). Mesoporous silica nanospheres (MSNs) were synthesized using an organic template method and then functionalized with aminopropyl groups through postsynthesis. After drug loading into the pores of aninopropyl functionalized MSNs (AP-MSNs), IND loaded AP-MSNs (IND-AP-MSNs) were encapsulated by ALG through the ionic interaction. The effects of surface chemical groups and ALG layer on IND release were systematically studied using scanning electron microscopy (SEM), transmission electron microscopy (TEM), nitrogen adsorption, zeta-potential analysis and TGA analysis. The surface structure and surface charge changes of the ALG encapsulated AP-MSNs (ALG-AP-MSNs) were also investigated. The results showed that sustained release of IND from the designed drug delivery system was mainly due to the blockage effect from the coated ALG. We believe that this combination will help designing oral sustained drug delivery systems for poorly water-soluble drugs.

* *Corresponding author.* Shenyang Pharmaceutical University, No. 103, Wenhua Road, Shenyang 110016, China. Tel./fax: +86 24 23986348.
E-mail addresses: silingwang@syphu.edu.cn, silingwang@hotmail.com (S. Wang).

1. Introduction

Oral delivery is the most convenient and easily accepted administration route for drugs. After oral administration, in order to be absorbed into the systemic circulation, a drug must first be dissolved in gastrointestinal fluids. However, for poorly water-soluble drugs, the dissolution is a rate-limiting step in drug absorption and, so, affects the oral bioavailability [1,2]. It is worth noting that nearly 40% of commercially available drugs or new drug candidates under development have poor water-solubility [3]. So, it is a great challenge to enhance the dissolution rate of poorly water-soluble drugs. Many strategies have been developed to solve this problem, such as nanotechnology and the use of solid dispersions, but the resulting formulations often suffer from poor stability.

In the past decade, mesoporous silica materials have attracted the attention of pharmaceutical researchers around the world. As we know, mesoporous silica materials have many unique properties, such as their non-toxic nature, large surface area and pore volume, tunable pore size, as well as chemically inert and easily modified surface properties [4–9]. Various types of such materials have been developed into drug delivery systems [10,11]. And these materials are considered very promising to solve the problems mentioned above. When loaded using mesoporous silica materials, the drug molecules can be separated on the surface of these materials, and therefore the intermolecular interactions of the crystal structure are prevented, which is the main reason why slow dissolution kinetics can be avoided [12–14]. In addition, the nano-scaled drug particles, which are in a higher free energy state, are confined in the rigid porous structure, making the drug nanoparticles more stable [14,15]. Therefore, employing mesoporous silica materials as drug carriers will enhance dissolution rate and stability of poorly water-soluble drugs. Moreover, the delivery rate enhancement provides a foundation for further study and investigation of the application of poorly water-soluble drugs to provide controlled or sustained delivery.

In order to improve patient compliance, drug efficacy and commercial value, it is better that the drug delivery rate is effectively controlled. And outer organic polymer coating has become one of effective ways to regulate the drug release pattern from mesoporous materials. H. Huang et al. have designed a new family of folate-decorated and carbon nanotube-mediated drug delivery system, and achieved a controlled release of the drug doxorubicin [16]. Lizhang Sun et al. have developed a novel chitosan encapsulated spherical nanosilica matrix as an oral sustained drug delivery system for poorly water-soluble drug carvedilol [15]. Chen Zhang et al. have described a new oral drug delivery system involving a combination of inorganic mesoporous material (CMK-5) and organic polymer poly dimethyl diallyl ammonium (PDDA), and achieved sustained drug release patterns for three different poorly water-soluble drugs [17]. Apparently, the outer organic polymer coat worked as a barrier to impede drug molecules diffusing from the pores of mesoporous silica materials into the outer environment. All these findings suggest that the combination of inorganic mesoporous silica materials and organic polymers may be a feasible and simple way to achieve sustained drug delivery.

Here, we have proposed a combination of inorganic mesoporous silica material, used as drug carriers, and a natural organic polymer ALG, to establish a sustained drug delivery system for poorly water-soluble drugs. Hence, mesoporous silica nanospheres (MSNs) were synthesized and functionalized by aminepropyl groups. IND, a BCS class II drug (poor water solubility and high biomenbrane permeability[18]), was chose as a model drug and loaded into the pores AP-MSNs. Then, the drug loaded AP-MSNs were encapsulated by ALG through the ionic interaction between the amine on MSNs and the carboxyl on ALG. Fig. 1 had illustrated the whole processes clearly. The structure features of samples, as well as the effects of surface chemical groups and the ALG layer on IND release, were systematically studied using SEM, TEM, nitrogen adsorption, zeta-potential analysis and TGA analysis. The surface structure and surface charge changes of the ALG encapsulated AP-MSNs (ALG-AP-MSNs) were also investigated via BET surface area measurement and zeta-potential measurement. We believe that this simple combination will help designing oral sustained drug delivery systems for poorly water-soluble drugs.

2. Materials and methods

2.1. Materials

Tetraethyl orthosilicate (TEOS), hexadecyl trimethyl ammonium bromide (CTAB), anhydrous ethanol (99.7%, AR), methanol dried (≧99.5%, AR) and sodium alginate (viscosity = 1.05~1.15 pas, the viscosity-average molecular weight = $1.30 \times 10^5 \sim 2.04 \times 10^5$, ALG) were obtained from Tianjin Bodi Chemical Holding Co., Ltd. Ethyl ether (≧99.0%, AR) and acetone (≧99.5%, AR) were produced by Tianjin Kaixin Chemical Industrial Co., Ltd. Indomethacin (purity >99.0%) was kindly supplied from Shijiazhuang Pharmaceutical Group (Huasheng Pharm. Co., Ltd.). All other chemicals were commercially available and were used as purchased without any further purification. Double distilled water was used in all experiments.

2.2. Preparation of MSNs and AP-MSNs

MSNs were synthesized according to the sol–gel method reported previously [19] with some modification. Briefly, 0.8 g CTAB was dissolved in the mixture of 100 ml water and 30 ml anhydrous ethanol under vigorous stirring at room temperature. Then 0.8 ml ammonia and 20 ml ethyl ether were added into the solution. When the solution became homogeneous, 2.5 ml TEOS was added dropwise into the solution. The solution was kept at room temperature for 4 h under vigorous stirring. The resulting precipitate was further homogenized using an ATS AH100D homogenizer (ATS Engineer Inc., China) at 800 bar for 20 cycles to reduce the aggregation of nanospheres. The white product was separated by centrifugation, washed using double distilled water and anhydrous alcohol for three times respectively, and dried at 60 °C over night. Finally, the product was calcined in air for 6 h to remove the template and other organic residues.

MSNs were functionalized with aminopropyl groups using the post-grafting method reported previously [20]. And the
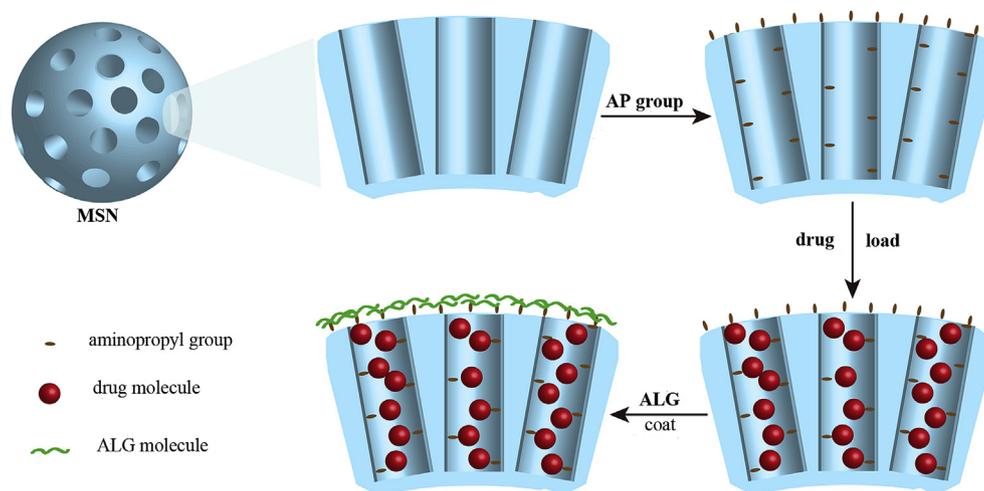
Fig. 1 – Schematic representation of aminepropyl functionalization of MSNs, IND loaded into AP-MSNs and ALG encapsulation.

obtained product was passed through the 80 mesh sieve and named as AP-MSNs.

2.3. Drug loading

The drug was loaded via the solvent deposition method, and accomplished as follows [12,14]. First, IND was dissolved in acetone in a sealed glass bottle (20 mg/ml), and then certain amount of the fabricated MSNs (or AP-MSNs) were added into the solution with the drug/silica mass ratio of 1:3. After gently stirred at room temperature over night, the mixture was dried at 35 °C in air for 24 h. Then washed in water for three times, the white sample was placed under reduced pressure for 48 h to remove the solvent completely. The products, named IND-MSNs and IND-AP-MSNs were passed through the 80 mesh sieve and placed in a vacuum dryer for further use.

2.4. The encapsulation of ALG

Firstly, 400 mg IND-AP-MSNs were dispersed in 20 ml double distilled water, and then an equal volume of the ALG solution (2 mg/ml) was added to the suspension and shaken at 80 rpm in a shaking incubator (THZ-82A, China) for 2 h under ambient condition. The encapsulated particles were collected by centrifugation at 4000 rpm for 10 min in a **centrifuge (TDL-6A, China) using "50 ml × 6" rotating disc**. The product was dried in air at 60 °C for 24 h, passed through the 80 mesh sieve and named as ALG-IND-AP-MSNs.

2.5. Morphology and structure characterization

The morphologies of products were observed using SUPRA-35 field emission SEM (ZEISS, Germany). Before analyzing, products were adhere to the double side adhesive carbon tape on an aluminum stub, and then gold-sprayed under vacuum condition. The porous structure features of the prepared samples were observed using a TEM (Tecnai G2 F30, FEI, The Netherlands). Prior to analysis, samples were dispersed in

double distilled water, and then being adsorbed on carbon-plated copper grids.

The pore size distributions, specific surface areas and total pore volumes were analyzed by an adsorption analyzer (Vsob-2800P, China). Prior to analysis, samples were degassed under vacuum at 60 °C for 6 h. The Brunauer-Emmett-Teller (BET) surface areas were calculated via experimental points at a relative pressure of $P/P_0 = 0.05$–0.25. The pore size distributions (D_{BJH}) were calculated from the desorption branch of isotherms via the Barrett-Joyner-Halenda (BJH) method. The total pore volumes were estimated from N2 amount adsorbed at a relative pressure of 0.9814.

2.6. The zeta-potential measurement

The zeta-potentials of MSNs and AP-MSNs, dispersed in double distilled water, were determined on a zeta potential instrument (Nano-zs90, USA). And each measurement was carried out in triplicate.

2.7. Drug loading analysis

The actual drug loadings were ascertained by extracting an accurately weighed amount of IND-loaded composites with methanol, followed by the determination of drug content using ultraviolet (UV) spectroscopy at a wavelength of 320 nm (UV-2000, Unico, USA). The standard curve was linear over the concentration range of 4.0–50.0 μg/ml. All measurements were carried out in triplicate.

2.8. TGA Analysis

To investigate the encapsulated ALG amount and exclude the interference of the drug content changes to the measurement, the TGA analysis of MSNs, AP-MSNs and ALG-AP-MSNs was carried out by TGA-50 instrument (Shimadzu, Japan) from 100 to 600 °C at the heating rate of 10 °C/min.

2.9. In vitro drug dissolution study

The drug dissolution patterns were studied using a USP II paddle method in a dissolution apparatus (ZRS-8G, Tianjin Tianda Tianfa Technology Co., Ltd.). The paddle speed was 100 rpm and the volume of the dissolution medium, kept the temperature at 37 ± 0.5 °C, was 900 ml. Phosphate buffer solution (pH = 6.8) was used as the dissolution medium. At appropriate sampling times, 5 ml samples were withdrawn and replaced by equal volume of fresh medium instantly. Each sample was filtered through a 0.22 μm membrane and tested using UV spectrophotometry (UV-2000, Unico, USA) at 320 nm. Each sample was equivalent to 25 mg IND and all the dissolution studies were carried out in triplicate.

2.10. Surface structure changes of ALG-AP-MSNs

In order to explore the state and the behavior of the ALG layer, when placed in the drug release media, the BET surface area measurement was carried out [15]. Briefly, six 50 ml. EP tubes were prepared and each Eppendorf (EP) tube was loaded with 60 mg of ALG coated blank AP-MSNs (ALG-AP-MSNs) and 30 ml pH 6.8 phosphate buffer solution. Then, after shaking for a selected time interval at 100 rpm, and 37 °C in a shaking incubator (AHZ-82A, China), one tube was taken out and the contents were separated by centrifugation at 4000 rpm and dried in air under 60 °C for 6 h. The specific surface area of the dried contents was then measured by an adsorption analyzer as mentioned above.

2.11. Zeta-potential changes of ALG-AP-MSNs in drug release media

To explore the interaction between the ALG layer and AP-MSNs during the drug release, zeta-potential changes of ALG-AP-MSNs in drug release media were measured. Briefly, 60 mg ALG-AP-MSNs were dispersed in 30 ml phosphate buffer solution (pH 6.8). And the suspension was shaken at 100 rpm, and 37 °C in a shaking incubator (AHZ-82A, China). At selected time intervals, the zeta-potential was measured according to the zeta-potential measurement section. Each measurement was carried out in triplicate.

3. Results and discussion

3.1. Morphology and structure characterization

As Fig. 2A and B showed, the synthesized spherical MSNs and AP-MSNs were nearly monodispersed with an average diameter of around 300 nm. From the TEM images of the MSNs, shown in Fig. 3A, we can see that the slit-like mesopores of MSNs were arranged radially, which would favor the mass diffusion. N_2 adsorption–desorption isotherms of MSNs, shown in Fig. 4, displayed a typical type IV feature with H4 hysteresis loops in accordance with the IUPAC classification [21], indicating a narrow slit-like pore structure, which agreed well with the results of TEM observation. It could be seen in Fig. 5 that MSNs had a pore size distribution at 2.3 nm and
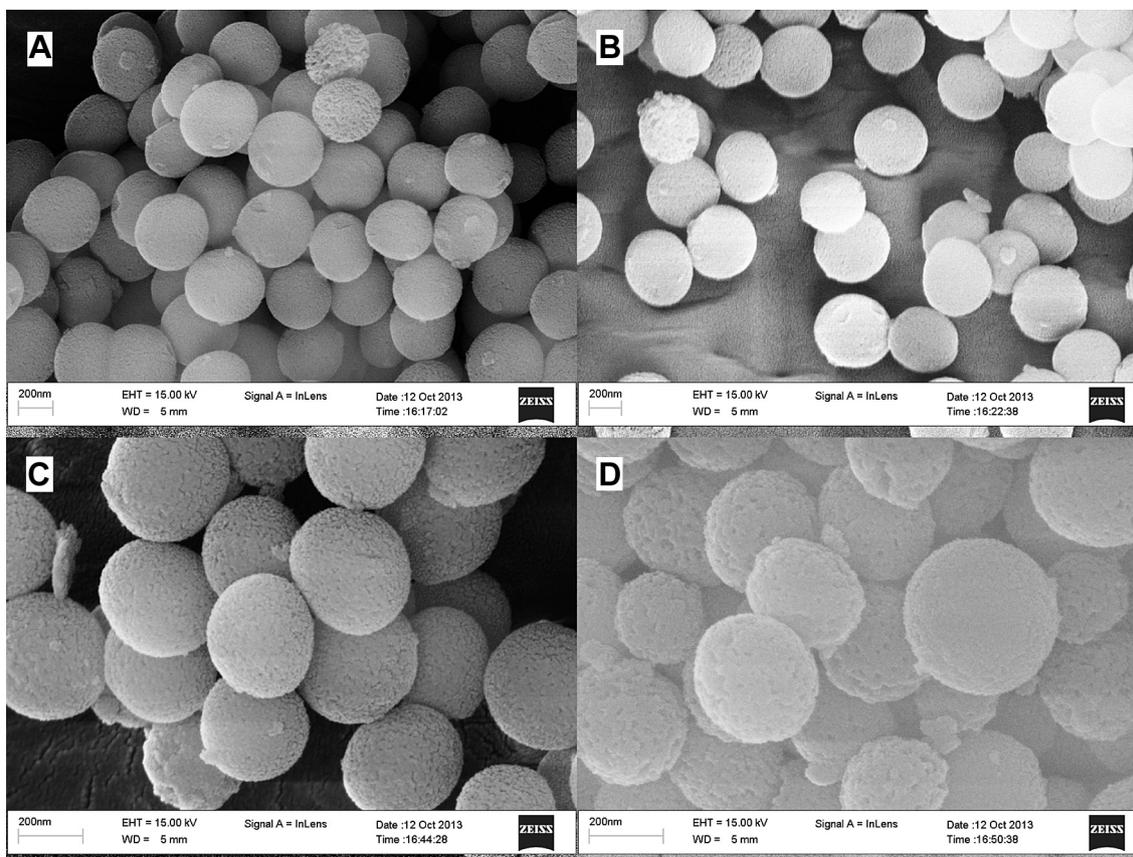

Fig. 2 – SEM images of (A) MSNs, (B) AP-MSNs, (C) IND-AP-MSNs and (D) ALG-IND-AP-MSNs.
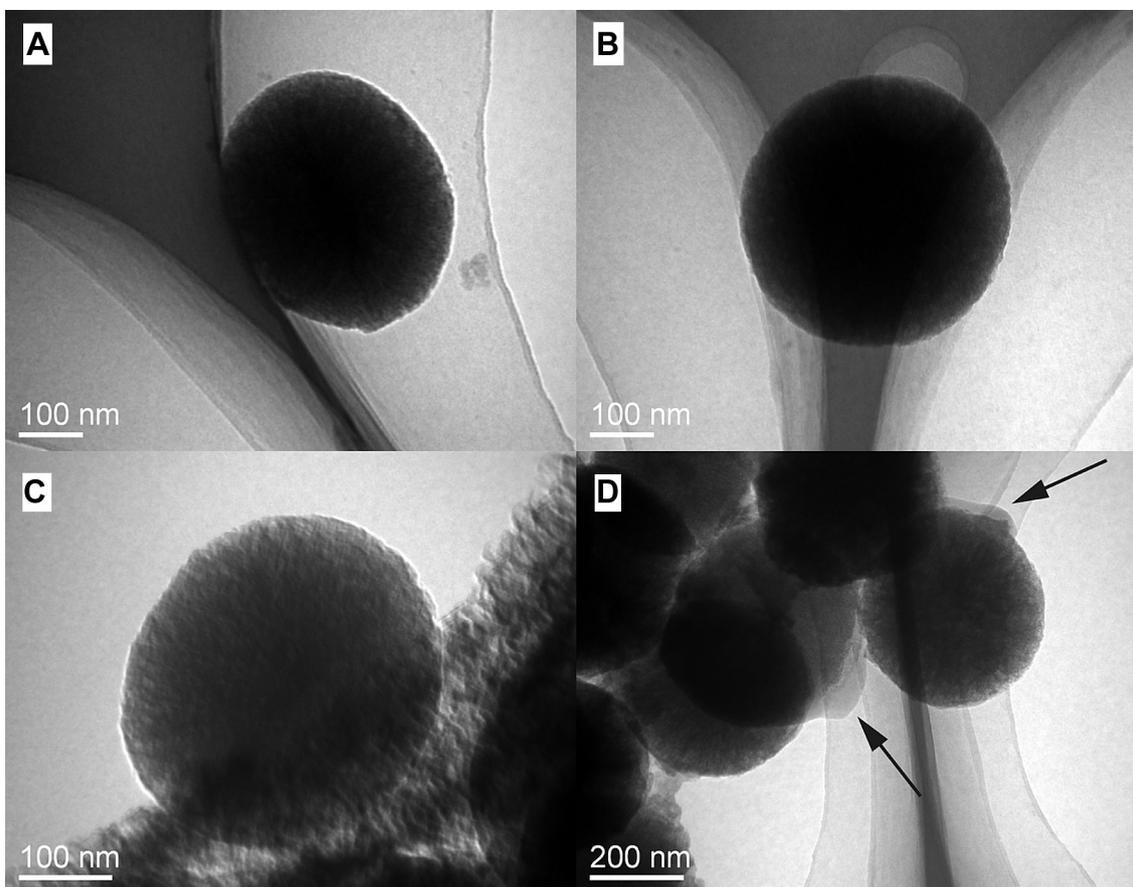
Fig. 3 – TEM images of (A) MSNs, (B) AP-MSNs, (C) IND-AP-MSNs and (D) ALG-IND-AP-MSNs.

3.8 nm. While, it should be interesting to notice that the pore size distribution line of AP-MSNs moved to the smaller direction slightly, which might be attributed to that the functionalized silane were attached to the pore surface. The synthesized MSNs had a high specific surface area of 1012.65 m^2/g and a large total pore volume of 0.81 cm^3/g. After functionalization, S$_{BET}$ and Vt were reduced, which also demonstrated the attachment of functionalized silane [20]. Although the adsorbed amount of nitrogen reduced, the shape of the hysteresis loop remained unchanged, which means that

the pore shape was not changed much by the postsynthesis approach. And it is in agreement with the TEM analysis, which is shown in Fig. 3B.

After drug loading and ALG coating, as shown in Fig. 2C and D, the nanospheres remained almost monodispersed. Compared with IND-AP-MSNs (shown in Fig. 3C), the edge of which looks very smooth, a thin layer could be seen at the edge of ALG-IND-AP-MSNs as the arrows pointed (shown in Fig. 3D), which should due to the ALG coating on IND-AP-MSNs. Moreover, after drug loading and ALG coating, S$_{BET}$
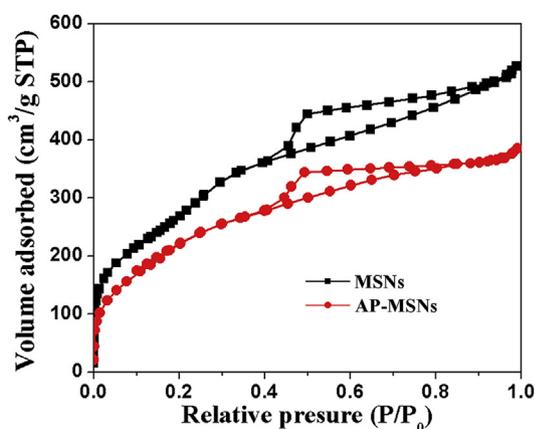

Fig. 4 – Nitrogen adsorption/desorption isotherms of MSNs and AP-MSNs.
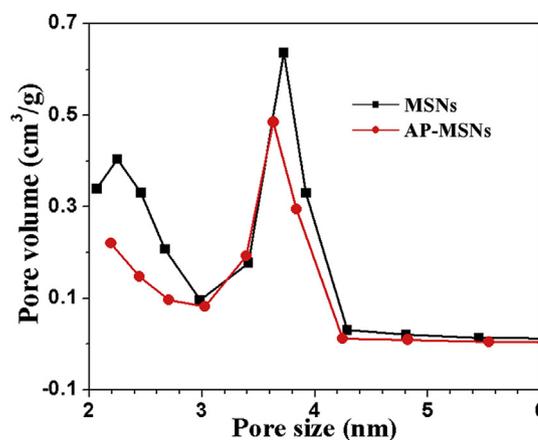

Fig. 5 – Pore size distributions of MSNs and AP-MSNs.

and Vt, as summarized in Table 1, were both sharply reduced. All these findings confirm the success of drug loading and ALG coating.

3.2. The zeta-potential measurement

In order to demonstrate the functionalization of aminopropyl groups on MSNs, we measured the zeta-potentials of MSNs and AP-MSNs. As Fig. 6 showed, the value of MSNs was −24.3 mV, while the zeta-potential increased to +12.0 mV after functionalization. This is because that the silanol groups were negatively charged easily under a wide range pH conditions [15,22], while the aminopropyl groups attached on MSNs were positively charged when placed in water [23]. The zeta-potential variation well demonstrated the successful functionalization of aminopropyl groups on MSNs. And the positively charged AP-MSNs would favor the following encapsulation of the polyanion ALG. It has been reported that the pKa values of the mannuronic acid and guluronic acid units of the ALG chain are 3.4 and 3.7, respectively [24]. So ALG was negatively charged under the encapsulating condition. And ALG could be encapsulated through the ionic interaction between the positively charged AP-MSNs and the negatively charged ALG.

3.3. Drug loading and characterization

IND was loaded according to the solvent deposition method, and then washed with water to remove the adsorbed drug on the outer surface of the carriers, so as to expose the aminopropyl groups for the subsequent ALG coating. And in order to compare the drug release patterns of IND-MSNs and IND-AP-MSNs, IND loaded MSNs were also washed with water. As shown in Table 1, UV measurement confirmed that the drug loading of IND could reach 18.31% for IND-MSNs and 16.44 for IND-AP-MSNs. However, during ALG coating process, some drug loaded in AP-MSNs was lost, so the drug loading for ALG-IND-AP-MSNs decreased to 12.73%.

3.4. TGA Analysis

In order to ascertain the encapsulated amount of alginate on the silica nanoparticles, the TGA analysis of MSNs, AP-MSNs
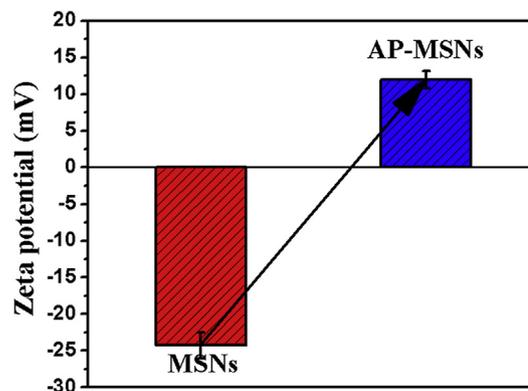

Fig. 6 – Zeta-potentials of MSNs and AP-MSNs.

and ALG-AP-MSNs was carried out. Because some drug might be lost during the encapsulating process, and the variation of the drug content will interfere with the analysis, so we induced this study using the samples without drug. For blank MSNs, shown in Fig. 7, the line was almost horizontal, suggesting that there was no organic residue in blank MSNs. The line for AP-MSNs decreased 2.7%, which should due to the weight loss of the functional groups. And the weight loss of the functional groups and the ALG layer was 16.6% for ALG-AP-MSNs. Therefore, we could calculate that the mass of the ALG layer account for 13.9% of the total mass of ALG-AP-MSNs.

3.5. In vitro drug release study

Fig. 8 showed the drug release profiles of raw IND, IND-MSNs, IND-AP-MSNs and ALG-IND-AP-MSNs in pH 6.8 release media. Compared with raw IND, IND-MSNs showed a much faster release pattern. The drug release within 2 h already reached more than 90%. The immediate drug release of IND-MSNs could be owing to the dispersing effect of MSNs with a high surface area and the hydrophilicity of mesoporous silica [12,14]. However, the drug release rate was a little slowed down for IND-AP-MSNs. Under the pH 6.8 drug release media,

Table 1 – Characteristics of drug carriers before and after drug uptake and after ALG encapsulation.

Sample	D_{BJH}[a] (nm)	S_{BET}[b] (m²/g)	Vt[c] (cm³/g)	Loading content efficiency (%)
MSN	2.3, 3.8	1012.65	0.81	
AP-MSNs	2.2, 3.6	852.42	0.60	18.31
IND-AP-MSNs		512.75	0.43	16.44
ALG-IND-AP-MSNs		328.91	0.34	12.73

[a] Dp is the pore diameter calculated by the BJH method on the branches of the nitrogen desorption isotherms.
[b] S_{BET} is the BET surface area calculated using experimental points at a relative pressure of $P/P_0 = 0.05 \sim 0.25$.
[c] Vt is the total pore volume determined at a relative pressure of 0.9814.
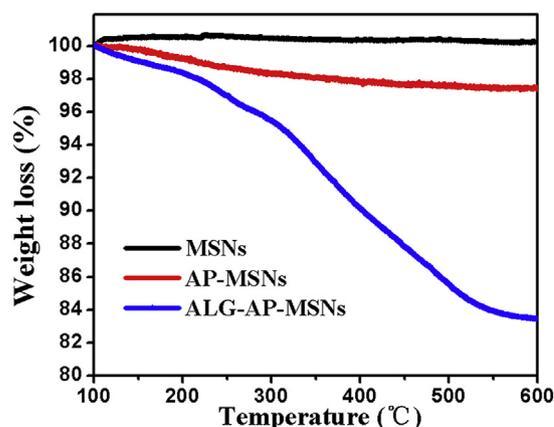

Fig. 7 – TGA patterns of MSNs, AP-MSNs and ALG-AP-MSNs.
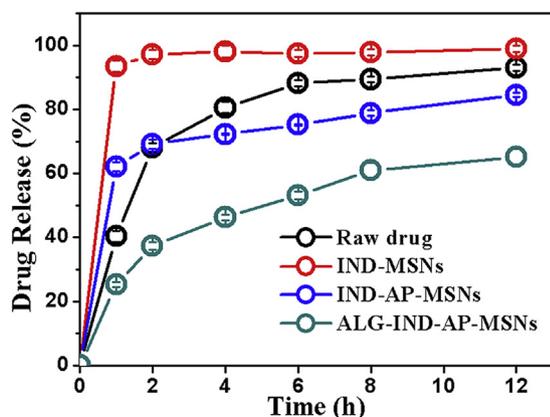
Fig. 8 – Drug release profiles of raw IND, IND-MSNs, IND-AP-MSNs and ALG-IND-AP-MSNs.

the aminopropyl groups on AP-MSNs should be positively charged, because AP-MSNs was already positively charged in double distilled water (pH about 7.0). And indomethacin molecules (pKa = 4.5) [25] were negatively charged. So there was ionic interaction between AP-MSNs and indomethacin, which could be used to explain why the drug release rate was slowed down to some extent. Moreover, the diffusion of the drug molecules also needed to overcome the hindrance of the alkyl chains in AP-MSNs [20]. In addition, ALG coated IND-AP-MSNs exhibited a more sustained drug release pattern. ALG was coated through the ionic interaction between the amine groups on the outer surface of the drug carrier and the carboxyl groups on ALG. The ALG layer performed a much strong blockage effect, and the drug release was effectively slowed down.

3.6. Surface structure changes of ALG-AP-MSNs

In order to explore the state and the behavior of the ALG layer, when placed in the drug release media, the BET surface area measurement was carried out in different time intervals. And to exclude the interference of the drug release to the
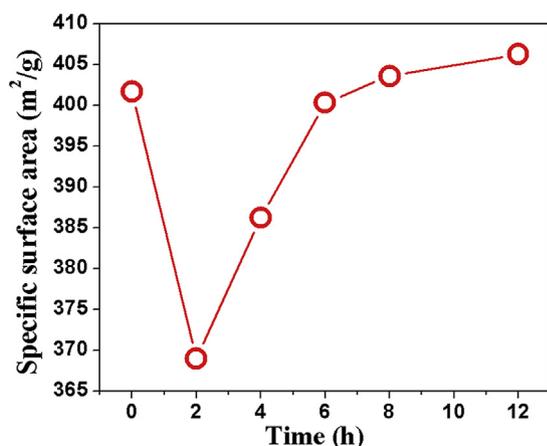
measurement, we induce this study using ALG coated blank AP-MSNs. From Fig. 9, we can see that the S_{BET} of ALG-AP-MSNs sharply decreased at the beginning, and gradually increase after that. The initial decrease might be caused by the swelling of the ALG layer. When touched with the pH6.8 release media, the carboxyl groups on ALG molecule was gradually ionized [25], making the molecule stretch and, so, the ALG molecule occupied more space and blocked the pores of the drug carrier. Meanwhile, the ALG layer might also be dissolved gradually in the media, which made the surface area value start to increase. When the dissolution behavior and the ionic interaction between the positively charged AP-MSNs and the negatively charged ALG reached a balance, the surface area tended to present no significant change. Therefore, a certain amount of swelled ALG retained on the drug carrier and hindered the drug molecules diffusing into the release media.

3.7. Changes of surface charge

The zeta-potentials of ALG-AP-MSNs in the drug release media were measured in different time intervals, so as to further investigate the interaction between the ALG layer and AP-MSNs during the drug release. As shown in Fig. 10, when contacting with the release media, the zeta-potential of ALG-AP-MSNs decreased to −7.97 mV, owing to the deionization of the carboxy groups on ALG molecule [25]. At this time, the deionization would cause the swelling of ALG molecule, induced by the repulsive force of the ionized carboxyl groups on ALG molecule. And the repulsive force between ALG molecules would lead to some ALG dissolved. So the zeta-potential started to increase. However, it should be notice that the zeta-potential kept in the negative throughout the whole study. This indicated that the ALG layer was not dissolved completely or detached from AP-MSNs, which might be attributed to the ionic interaction between the positively charged amino groups on AP-MSNs and the negatively charged carboxy groups on the ALG layer. Therefore, the drug release would be hindered by the ALG layer throughout the whole drug release process.
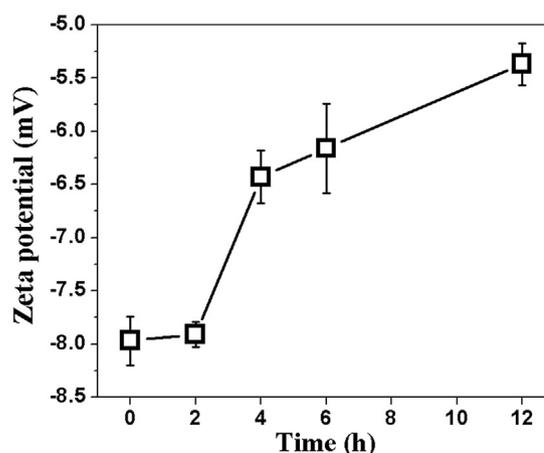

Fig. 9 – BET surface area changes at different sampling times.

Fig. 10 – Surface charge changes at different sampling times.

4. Conclusion

In summary, we have successfully developed an effective way to control the drug release rate of a poorly water-soluble drug and eventually obtained a sustained drug delivery system for the poorly water-soluble drug indomethacin. MSNs were functionalized by aminopropyl groups and used as drug carriers. To control the drug release rate, a natural polymer ALG was coated on the drug loaded AP-MSNs through ionic interaction. The blockage effect of the ALG layer could effectively slow down the drug release. Therefore, we believe this simple strategy will have potential applications in producing sustained drug systems for poorly water-soluble drugs. Also, this combination of mesoporous silica materials and ALG coating will expand the applications of inorganic materials and polymers.

Acknowledgments

REFERENCES

[1] Lipinski CA, Lombardo F, Dominy BW, et al. Experimental and computational approaches to estimate solubility and permeability in drug discovery and development settings. Adv Drug Deliv Rev 1997;23:3–25.

[2] Lipinski CA. Poor aqueous solubility – an industry wide problem in ADME screening. Am Pharm Rev 2002;5:82–85.

[3] Liu Y, Sun C, Hao Y, et al. Mechanism of dissolution enhancement and bioavailability of poorly water soluble celecoxib by preparing stable amorphous nanoparticles. J Pharm Pharm Sci 2010;13:589–606.

[4] Liu Y, Zhang W, Pinnavaia TJ. Steam-stable aluminosilicate mesostructures assembled from zeolite type Y seeds. J Am Chem Soc 2000;122:8791–8792.

[5] Liu Y, Zhang W, Pinnavaia TJ. Steam-stable MSU-S aluminosilicate mesostructures assembled from zeolite ZSM-5 and zeolite beta seeds. Angew Chem Int Ed 2001;40:1255–1258.

[6] Han Y, Li D, Zhao L, et al. High-temperature generalized synthesis of stable ordered mesoporous silica-based materials by using fluorocarbon-hydrocarbon surfactant mixtures. Angew Chem 2003;115:3761–3765.

[7] Munoz B, Ramila A, Perez-Pariente J, et al. MCM-41 organic modification as drug delivery rate regulator. Chem Mater 2003;15:500–503.

[8] Barbe C, Bartlett J, Kong L, et al. Silica particles: a novel drug-delivery system. Adv Mater 2004;16:1959–1966.

[9] Lai C-Y, Trewyn BG, Jeftinija DM, et al. A mesoporous silica nanosphere-based carrier system with chemically removable CdS nanoparticle caps for stimuli-responsive controlled release of neurotransmitters and drug molecules. J Am Chem Soc 2003;125:4451–4459.

[10] Yang P, Gai S, Lin J. Functionalized mesoporous silica materials for controlled drug delivery. Chem Soc Rev 2012;41:3679–3698.

[11] Uejo F, Limwikrant W, Moribe K, et al. Dissolution improvement of fenofibrate by melting inclusion in mesoporous silica. Asian J Pharm Sci 2013.

[12] Hu Y, Wang J, Zhi Z, et al. Facile synthesis of 3D cubic mesoporous silica microspheres with a controllable pore size and their application for improved delivery of a water-insoluble drug. J Colloid Interface Sci 2011;363:410–417.

[13] Mellaerts R, Aerts CA, Van Humbeeck J, et al. Enhanced release of itraconazole from ordered mesoporous SBA-15 silica materials. Chem Commun 2007:1375–1377.

[14] Hu Y, Zhi Z, Wang T, et al. Incorporation of indomethacin nanoparticles into 3-D ordered macroporous silica for enhanced dissolution and reduced gastric irritancy. Eur J Pharm Biopharm 2011;79:544–551.

[15] Sun L, Wang Y, Jiang T, et al. Novel chitosan-functionalized spherical nanosilica matrix as an oral sustained drug delivery system for poorly water-soluble drug carvedilol. ACS Appl Mater Inter 2012;5:103–113.

[16] Huang H, Yuan Q, Shah J, et al. A new family of folate-decorated and carbon nanotube-mediated drug delivery system: synthesis and drug delivery response. Adv Drug Deliv Rev 2011;63:1332–1339.

[17] Zhang C, Zhao Q, Wan L, et al. Poly dimethyl diallyl ammonium coated CMK-5 for sustained oral drug release. Int J Pharm 2014;461:171–180.

[18] Amidon GL, Lennernäs H, Shah VP, et al. A theoretical basis for a biopharmaceutic drug classification: the correlation of in vitro drug product dissolution and in vivo bioavailability. Pharm Res 1995;12:413–420.

[19] Du X, He J. Fine-tuning of silica nanosphere structure by simple regulation of the volume ratio of cosolvents. Langmuir 2010;26:10057–10062.

[20] Zhang Y, Zhi Z, Jiang T, et al. Spherical mesoporous silica nanoparticles for loading and release of the poorly water-soluble drug telmisartan. J Control Release 2010;145:257–263.

[21] Pierotti R, Rouquerol J. Reporting physisorption data for gas/solid systems with special reference to the determination of surface area and porosity. Pure Appl Chem 1985;57:603–619.

[22] Lvov Y, Ariga K, Onda M, et al. Alternate assembly of ordered multilayers of SiO2 and other nanoparticles and polyions. Langmuir 1997;13:6195–6203.

[23] Yang Y-J, Tao X, Hou Q, et al. Mesoporous silica nanotubes coated with multilayered polyelectrolytes for pH-controlled drug release. Acta Biomater 2010;6:3092–3100.

[24] Liu X, Xue W, Liu Q, et al. Swelling behaviour of alginate-chitosan microcapsules prepared by external gelation or internal gelation technology. Carbohyd Polym 2004;56:459–464.

[25] Somasundaram S, Rafi S, Hayllar J, et al. Mitochondrial damage: a possible mechanism of the "topical" phase of NSAID induced injury to the rat intestine. Gut 1997;41:344–353.